Second-order chromatographic photochemically-induced fluorescence emission data coupled to chemometric analysis for the simultaneous determination of urea herbicides in the presence of matrix co-eluting compounds

Juan A. Arancibia and Graciela M. Escandar*

Instituto de Química Rosario (CONICET-UNR), Departamento de Química Analítica. Facultad de Ciencias Bioquímicas y Farmacéuticas, Universidad Nacional de Rosario, Suipacha 531 (2000) Rosario, Argentina. E-mail: escandar@iquir-conicet.gov.ar

This paper presents a novel approach for the simultaneous determination of isoproturon, rimsulfuron and monuron, three widely used urea-derivative herbicides, in interfering environmental samples, combining the advantages of photoinduced fluorescence (PIF) emission, liquid chromatography and second-order chemometric algorithms. Chromatographic detection is made with a fast-scanning spectrofluorimeter, which allowed the efficient collection of PIF through a post-column photoreactor. Thus, second-order elution time-PIF emission data matrices are rapidly obtained (in less than 4 min) with a chromatographic system operating in isocratic regime using a minimal amount of organic solvent. The goal of the present study was the successful resolution of a system in the presence of foreign compounds which can be present in real samples. The study was employed for the discussion of the scopes of the applied second-order algorithms selected for data processing, namely parallel factor analysis (PARAFAC), multivariate curve resolution-alternating least-squares (MCR-ALS), and multidimensional and unfolded partial least-squares coupled to residual bilinearization (N- and U-PLS/RBL). U-PLS/RBL showed the best performance to quantify the herbicides, even when the foreign compounds showed very similar spectral and time profiles to the analytes. The quality of the proposed technique was assessed on the basis of the analytical recoveries from different types of water samples spiked with analytes and other selected agrochemicals. After a solid-phase extraction, reaching a preconcentration factor of 50, detection limits of 2.9, 2.4, and 1.7 ng mL^{-1} for isoproturon, rimsulfuron, and monuron, respectively, were obtained in those interfering matrices, with relative prediction errors lower than 5 %.

Introduction

Herbicides belonging to the urea family are extensively used for the control of broad-leaved weeds and grasses in a wide range of crops.[1] Both the water solubility and the persistence (*ca.* weeks or months) of these herbicides explain their frequent presence in soils and natural waters.[2] Some of them have also been detected in different surface and groundwaters of European countries [3–5] at levels higher than the maximum permissible concentration proposed by the European Drinking Water Directive 98/83 (0.1 ng mL^{-1} for any individual pesticide, and 0.5 ng mL^{-1} for the total pesticide content).[6]

Among substituted-urea herbicides, isoproturon (ISO; [3-(4-isopropylphenyl)-1,1-dimethylurea]; Fig. 1) is included in the list of priority compounds of the European Water Framework Directive,[7] and represents one of the targets of the present study. ISO is extensively used in European cereal production,[8] and it is often found in contaminated European groundwaters, surface waters**,** and effluents.[9] Due to the presence of ISO in rivers in the UK it had to be removed from the market during 2009.[10] A study of water pollution by herbicides in Germany revealed that more than three quarters of the total herbicide load of the effluents of the rural waste water treatment plant consisted of ISO, with a maximum concentration of 42 ng mL^{-1}.[11] A monitoring study for polar pollutants in European river waters indicated that the single highest ISO concentration was approximately 2 ng mL^{-1}.[12]

In addition to ISO, two frequent herbicides, the sulfonylurea derivative rimsulfuron (RIM; [1-(4,6-dimethoxy-2-pyrimidinyl)-3-[3-(ethylsulfonyl)-2-pyridylsulfonyl]urea]) and the phenylurea derivative monuron (MONU; [3-(*p*-chlorophenyl)-1,1-dimethylurea]) were included in our investigation (Fig. 1). RIM is one of the most used herbicide for potato crops, and has adverse effects in earthworms, non-target terrestrial and aquatic plants.[13] MONU has been reported to be possibly carcinogenic in humans and its use has been banned in USA.[14]

Although liquid chromatography-mass spectrometry methods are the most commonly applied ones for the determination of contaminants and pesticides in general,[15] the fact that both sulfonyl- and phenylurea herbicides display photoinduced fluorescence (PIF) upon UV radiation has allowed the development of green methods for their quantification based on this type of signal.[16,17]

The coupling of either high performance liquid chromatography (HPLC) or flow-injection analysis (FIA) with on-line PIF detection was previously applied for the automated analysis of phenylurea herbicides.[17,18–20] Very recently, two urea-herbicides, fenuron and diflubenzuron, were determined by direct-laser-PIF.[21] However, in all of these works the presence of interfering agents represents a problem, especially in those cases where the limit of tolerance for the interference is very low.

The lack of selectivity of a method due to the presence of interferences can be easily overcome if the analysis is assisted by multi-way calibration. This type of calibration uses higher-order data, and allows the prediction of component concentrations in the presence of any number of unsuspected constituents which can be present in real samples. This useful property is named the "second order advantage", and avoids the requirement of either interference removal, as in zeroth-order calibration, or the construction of a large and diverse calibration set, as in first-order calibration.[22–25] Interference removal extends the analysis time and the experimental work, and frequently involves the use of significant amounts of polluting organic solvents, in contrast to the green analytical chemistry principles.[26,27]

In this paper, higher-order data were obtained coupling HPLC, under an isocratic regime, to a fast scanning fluorescence (FSF) detector able to rapidly detect the PIF signals produced by rimsulfuron, monuron and isoproturon, which are post-column irradiated with UV light. Thus, the elution time–photoinduced fluorescence matrix (ET-PIFM) data are obtained in short times and using minimal solvent volumes. The determinations are carried out in

solutions containing the analytes and additional agrochemicals selected as potential interferences, namely 2-methyl-4-chlorophenoxyacetic acid (MCPA), thiabendazole (TBZ), fuberidazole (FBZ) and carbaryl (CBL) (Fig. 1). The latter compounds showed PIF spectra significantly overlapped with those of the studied analytes. Since the former agrochemicals are usually employed in our geographical region, they may also be present in real water samples.

Four chemometric algorithms which achieve the second order advantage, i.e., parallel factor analysis (PARAFAC)[28] unfolded partial least-squares coupled to residual bilinearization (U-PLS/RBL)[29,30], multidimensional partial least-squares coupled to residual bilinearization (N-PLS/RBL),[31] and multivariate curve resolution-alternating least-squares (MCR-ALS)[32] were applied to process the ET-PIFMs. In those samples containing foreign species, which are closer to real cases, notable differences in the prediction capabilities of the employed algorithms were observed and discussed.

It is important to remark that few works using the present HPLC-FSF approach coupled to second-order calibration have been reported in the literature.[33–36] To the best of our knowledge, this is the first time that the potentiality of the second-order advantage is evaluated using ET-PIFMs. Finally, the feasibility of determining the three herbicides in natural water samples is demonstrated.

Experimental

Reagents and solutions

All reagents were of high-purity grade and used as received. Isoproturon, rimsulfuron, monuron, MCPA (2-methyl-4-chlorophenoxyacetic acid), mecoprop (methylchlorophenoxypropionic acid), 2,4D (2,4-dichlorophenoxyacetic acid), dichlorprop [(R)-2-(2,4-dichlorophenoxy)propanoic acid], dicamba (3,6-dichloro-2-methoxybenzoic acid), linuron [3-

(3,4-dichlorophenyl)-1-methoxy-1-methylurea], neburon [1-butyl-3-(3,4-dichlorophenyl)-1-methylurea], diuron [3-(3,4-dichlorophenyl)-1,1-dimethylurea], chlorsulfuron [1-(2-chlorophenylsulfonyl)-3-(4-methoxy-6-methyl-1,3,5-triazin-2-yl)urea], thiabendazol (TBZ), sodium dodecylsulfate (SDS), hexadecyltrimethylammonium chloride (HTAC), fuberidazol (FBZ), carbaryl (CBL), and citrate buffer were purchased from Sigma-Aldrich (Milwaukee, WI, USA). Acetonitrile and methanol were purchased from Merck (Darmstadt, Germany). Water was purified using a MilliQ system (Millipore, Bedford, USA).

Stock solutions of herbicides were prepared in methanol and stored in dark flasks at 4 °C. In these conditions, solutions were stable for at least three months. Working samples were prepared as indicated below.

Instrumentation and procedure

Chromatographic measurements were carried out on an Agilent 1200 Series instrument (Agilent Technologies, Waldbronn, Germany), controlled by the ChemStation software package, and a Varian Cary-Eclipse luminescence spectrometer (Varian, Mulgrave, Australia) as detector. A 200 µL loop was employed to introduce each sample onto an Agilent Eclipse XDB-C18 column (5 µm average particle size, 150 mm × 4.6 mm i.d.). A photoreactor, consisting of a polytetrafluoroethylene (PTFE) tube network (3 m × 0.8 mm i.d.) coiled around an 8 W mercury lamp, was used for the post-column photoirradiation. The mobile phase consisted of a mixture of acetonitrile, citrate buffer (pH 6.0) and methanol (55:40:5, v/v) flowing at 1 mL min^{-1}. Chromatographic elution, performed under an isocratic regime, was accomplished in approximately 4 min. The column temperature was set at 25 °C. The pH of solutions was measured with a Metrohm (Herisau, Switzerland) 713 potentiometer equipped with a combined glass electrode.

ET-PIFMs were collected with the excitation wavelength fixed at 272 nm, using emission wavelengths from 288 to 460 nm each 3 nm and times from 0 to 4 min each 1.4 s. The excitation and emission slit widths were 10 nm and photomultiplier sensitivity was 800 V. The emission-time matrices were saved in ASCII format and transferred to a PC based on AMD Sempron 2800 for subsequent manipulation.

Calibration, validation and test samples

A calibration set of 15 samples containing the studied herbicides at the concentrations provided by a central composite design for three factors and five levels by factor was prepared (Table 1). The concentration ranges were: 0–4 μg mL^{-1} (isoproturon), 0–5 μg mL^{-1} (rimsulfuron), and 0–3 μg mL^{-1} (monuron). Linearity was corroborated within these values, and no efforts were made in order to find the upper linear limits.

A validation set was prepared employing concentrations different than those used for calibration and following a random design (Table 1). Calibration and validation samples were prepared by measuring appropriate aliquots of standard solutions, placing them in 5.00 mL volumetric flasks, and completing to the mark with the solvent mixture used as mobile phase and HTAC solution in order to obtain a 0.011 mol L^{-1} HTAC final concentration.

With the purpose of evaluating the proposed strategy in the presence of potential interferences, additional test samples containing the three studied herbicides and TBZ, FBZ, CBL, and MCPA used as potential interferences were prepared. Agrochemicals selected as potential interferents were added at different ratios in the following ranges: 0.3–0.5 μg mL^{-1} (TBZ), 0.04–0.06 μg mL^{-1} (FBZ), 0.8–1.2 μg mL^{-1} (CBL), and 7–10 μg mL^{-1} (MCPA).

Water sample procedure

Tap, river, and underground water samples were prepared by spiking each sample with standard solutions of the studied herbicides, obtaining concentration levels in the range 0.01–0.05 μg mL^{-1} for each of them. In addition, the potential interferences (FBZ, TBZ, CBL or MCPA) were also incorporated to these samples at concentrations between 4×10^{-3} and 7 μg mL^{-1}. These water samples were prepared in duplicate. Because of the low investigated concentrations of analytes, solid-phase extraction (SPE) had to be applied before the determination. The SPE procedure was carried out using Empore Octadecyl C18 membranes purchased from Supelco (Bellefonte, PA, USA). Prior to the extraction of 50 mL of the sample, the membrane was conditioned with 1 mL of methanol. The retained analytes were eluted with 1 mL of mobile phase containing HTAC. This sample was then subjected to the same chromatographic analysis as the validation samples. In this way, the preconcentration factor was 50. This factor could be easily increased by one order of magnitude or even more, simply by increasing the volume of treated water.

Chemometric Algorithms and Software

The theory of the applied algorithms is well documented and a brief description can be found in the Supplementary Data. The routines employed for PARAFAC, MCR-ALS, N-PLS, N-PLS/RBL, U-PLS and U-PLS/RBL are written in MATLAB 7.0. All algorithms were implemented using the graphical interface of the MVC2 toolbox, which is available on the Internet. [37]

Results and discussion

Urea herbicide photoproducts

The studied herbicides were found to be naturally non-fluorescent in neither aqueous nor organic solvents, whereas significant fluorescence bands appeared upon UV irradiation, suggesting the formation of photoproducts (Fig. 2A).

On the basis of fluorescence spectral comparisons, some authors have concluded that structures similar to aniline and substituted anilines may be responsible for the fluorescence of phenylurea (ISO and MONU) photoproducts.[38,39]

In the case of RIM, the sulfonylurea bridge (Fig. 1) is quite labile and can be photochemically cleaved on both sides of the carbonyl, yielding an aryl sulfonamide and a nitrogen-containing heterocycle derived from pyrimidine[16]. Since this heterocyclic product is non-fluorescent, it is likely that the aryl sulfonamide moiety is responsible of the observed fluorescence.[16]

Surfactants and pH effects on the fluorescence signals

As previously reported, the presence of surfactants such as SDS and HTAC at concentrations higher than their critical micellar concentrations (8.1×10^{-3} and 1.3×10^{-3} mol L^{-1}, respectively, ref. 40) has a significant influence on the PIF intensity of different pesticides.[16,39,41] Preliminary experiments showed that the addition of HTAC to the samples provided signal enhancements larger than SDS and, therefore, HTAC was selected for subsequent studies.

Coly et al.[16] demonstrated that pyrimidine-based herbicides (like rimsulfuron) exhibit PIF signals at pH values ranging between 2 and 8, whereas adequate signals were obtained using pH 6–7 in the phenylurea systems.[17] Our exploratory experiments proved that a pH = 6, given for example by citrate buffer, produced satisfactory signals and it was selected for the present experiments.

Optimization of chromatographic conditions

According to previous experience related to the chromatographic determination of urea derivative herbicides,[17] mobile phases containing different ratios of acetonitrile and buffer solution were tested. In addition, it was found that methanol at concentrations about 5 % improves the intensity and quality of the peaks. Higher percentages of methanol (10–15 %) did not produce any changes. In conclusion, the mobile phase constituted by acetonitrile-citrate buffer and methanol in a 55:40:5 ratio provided the best PIF bands and it was used in all runs.

In a chromatographic-PIF system, for each sample volume there is an optimum irradiation time which depends on the flow rate and on the length of the photoreactor. For the three sample volumes assayed (20, 50 and 200 μL), three photoreactor lengths (100, 300 and 600 cm) and flow rates in the range 0.8 and 1.5 mL min^{-1} were probed. It was corroborated that a 300 cm photoreactor length, a flow rate of 1 mL min^{-1}, and 200 μL of injection volume produced the most sensitive signals. Under these latter conditions the three herbicides elute in less than 4 min.

A summary of the experimental conditions applied for the determination of the evaluated herbicides is given in Table 2.

Multivariate calibration results

Figs. 3A,B show a three-dimensional and a contour plot, respectively, of an ET-PIFM for a mixture of the three studied herbicides. It is verified that overlapping occurs between the signals of RIM and MONU, and as will be discussed below, the situation becomes more serious if additional agrochemicals which may overlap with any of the peaks (Figs. 3C,D) are also present. In this latter case, it is highly convenient the use of second-order calibration

with suitable algorithms for the quantitation of the analytes, because of the need of achieving the second-order advantage.

Two problems are known to be present when elution time-fluorescence emission second-order data are acquired: (1) the measurement of an emission spectrum of a flowing sample, which makes the sample concentration variable during spectral detection, and (2) the lack of repeatability in the elution time profiles between successive runs[33]. The first problem is overcome using a fast-scanning detector which allows spectra to be obtained in a very short time (at a scanning rate of 14,400 nm s^{-1} the recording time is significantly lower than the width of a typical chromatographic band). As regards the second issue, it was observed that chromatographic band shifts between consecutive runs were not significant when validation samples (without foreign compounds) were measured (Fig. 4). However, in the presence of additional compounds which strongly overlap both in the spectral and time modes, slight shifts of the analyte bands are verified between different runs, making the data non-trilinear.

In order to compare the ability of different algorithms towards these data, both validation and test samples were processed with algorithms which require trilinearity (PARAFAC) or which are more flexible in this regard (MCR-ALS, U-PLS/RBL, and N-PLS/RBL).

Validation samples

With the purpose of building a second-order calibration model for analyte quantitation, ET-PIFMs were recorded for the calibration samples (see Table 1). After a suitable consideration of the regions corresponding to maximum signals, the selected working ranges were: 2–4 minutes (elution time) and 288–399 nm (PIF emission).

The number of components when PARAFAC was applied was selected by the so-called core consistency diagnostic,[42] which consists of studying the structural model based on the data and the estimated parameters of gradually augmented models. A PARAFAC model is

considered to be appropriate if incorporating an additional component does not considerably improve the fit.[42] The number of components was also analysed considering both the spectral and the chromatographic profiles produced by the addition of subsequent components. In the latter test, if the addition of a new component generated repeated analyte profiles, the new component was discarded and the previous number of components was selected. The number of responsive components in validation samples obtained using both procedures was three. The number of components could be justified by the presence of three different signals corresponding to each evaluated analyte.

PARAFAC was initialized with the loadings given by the best fit after a small number of trial runs, selected from the comparison of the results provided by generalized rank annihilation and several random loadings.[43] It is known that PARAFAC allows to obtain physically meaningful profiles. Indeed, the time and spectral profiles retrieved by PARAFAC for a typical validation sample are very similar to those corresponding to the experimental ones (see Fig. S1 in Supplementary Data).

Fig. 5A shows the prediction results corresponding to the application of this algorithm to a set of 12 validation samples, different from those used for the calibration step. As can be observed, the predictions for the three analytes are in good agreement with the corresponding nominal values. If the elliptical joint confidence region (EJCR)[44] is analyzed for the slope and intercept of the above plot (Fig. 5E), we conclude that ellipses include the theoretically expected value of (1,0), indicating the accuracy of the applied methodology.

MCR-ALS was performed with matrix augmentation in the temporal direction, because this direction should be the one corresponding to potential profile changes. The number of components was estimated from the plot of singular values as a function of a trial number of components, locating a number for which the plot stabilizes. The latter number is initially employed for MCR-ALS analysis, and is afterwards refined (increased or decreased) until an

appropriate solution is found, with a reasonable least-squares fit and physically recognizable profiles. For a given number of responsive components, their spectra were then estimated from the analysis of the so-called purest variables, extracting the purest spectra of the mixture from a series of spectra of mixtures of varying composition.[45] The profiles provided by the latter analysis were suitable to perform the resolution and, therefore, it was not necessary to include reference spectra for the analyte as initial estimates for MCR-ALS. In the studied system, the number of MCR components was four, and they were ascribed to the three analytes and the background.

During the iterative procedure leading to chemically recognizable solutions, non-negativity constraints in both data modes and unimodality in the temporal mode were applied. The selected MCR convergence criterion was 0.1% (relative change in fit for successive iterations) and convergence was achieved after less than 20 iterations in most of the evaluated samples. The good quality of the MCR-ALS recovered profiles for validation samples can be appreciated in Fig. 2S of Supplementary Data, and the corresponding results, also of high quality, are shown in Figs. 5B and 5E.

Finally, algorithms based on latent variables (N- and U-PLS/RBL) were applied to validation samples. In contrast to PARAFAC and MCR-ALS, these algorithms do not render approximations to pure constituent profiles and thus the chemical interpretability is lost. However, these methodologies show a great flexibility and, as will be demonstrated below, they are able to cope with some data sets deviating from trilinearity.

The optimum number of factors for modelling the calibration set, obtained applying the cross-validation method described by Haaland and Thomas,[46] was three for ISO and RIM, and two for MONU. Figs. 5C-D show the good prediction results corresponding to the application of N-PLS and U-PLS to validation samples, and Fig. 5E displays the corresponding EJCR tests.

The analytical performances for the four selected algorithms applied to validation set can be appreciated from the statistical results shown in Table 3. These results are promising, taking into account that the simultaneous determination of the three herbicides is rapidly carried out using the entire chromatographic data matrices.

Test samples

The usefulness of the proposed method could not be completely appreciated until its ability to overcome the ubiquitous problem of the potential presence of interfering species in the analyzed matrices is demonstrated. The selection of potential interferences which could be concomitantly present in the samples was carried out evaluating the analytical responses of different agrochemicals subjected to the same working conditions used in the current determination. It was verified that mecoprop, 2,4D, dicamba, linuron, neburon, diuron, chlorsulfuron, and dichlorprop are either not fluorescent or only produce very weak fluorescence signals. On the other hand, the phenoxy herbicide MCPA, the fungicides TBZ and FBZ, and the insecticide CBL coelute with the analytes under the established working conditions and also strongly overlap the spectral signals of the three studied herbicides (Fig. 2B). Therefore, test samples containing these compounds were prepared and analysed.

Applying the same procedure as for validation samples, our first attempt was to carry out the quantification using the complete data matrices involving the full range of both elution times and emission wavelengths. However, preliminary studies performed with all selected algorithms showed that it was not possible to obtain reliable results working with the whole ranges. Therefore, the specific time-spectral region was systematically varied in the proximities of the maximum signal for each analyte, selecting the parameters which rendered the best statistical indicators. The final elution time and emission wavelength ranges were:

3.14 min–3.74 min and 288 nm–399 nm for ISO, 2.15 min–2.68 min and 288 nm–375 nm for RIM, and 2.82 min–3.35 min and 333 nm–405 nm for MONU.

The selection of the number of PARAFAC factors was carried out through the same tests as in the validation samples. Depending on the investigated region, the estimated number of components varied between two and four. As can be appreciated in Fig. 6A, the recovery results corresponding to the application of PARAFAC to samples containing potential interferents show some dispersion of the predictions with respect to the perfect fit. This fact may be explained considering both: (1) the significant spectral overlapping among the analytes and interferences (see Fig. 2B) which precludes the successful decomposition of the three-way, and (2) the variation of elution times of the analytes from run to run, verified in these complex matrices due to a sample matrix effect (Fig. 4), which produces a slight loss of data trilinearity.

MCR-ALS is very useful for calibration with data involving changes in constituent profiles along one of the instrumental data modes (e.g. elution time mode), as in the present case. Therefore, an augmented matrix along the elution time direction was built and processed by the algorithm. As in validation samples, the number of MCR components was estimated from the plot of singular values as a function of principal component number. The algorithm was initialized from the analysis of the so-called purest variables, and constraints of non-negativity in both data modes and unimodality in the temporal mode were applied, with a selected MCR convergence criterion of 0.1%.

The predicted concentrations (Fig. 6B) are rather poor in relation to the nominal values, and this result was ascribed to the significant spectral similarity among analytes and interferents.

It is important to point out that although the EJCRs for PARAFAC and MCR-ALS in Fig. 6 include the theoretically expected 1,0 values, the ellipse sizes are unsuitably large. This

conclusion is also corroborated by the statistical analysis of Table 3, where high REP values are calculated in test samples when these algorithms are employed.

When N- and U-PLS/RBL algorithms were applied to the test samples, in addition to the number of latent variables estimated for the calibration set for ISO, RIM and MONU in the corresponding selected regions, these samples required the introduction of the RBL procedure. In most samples, two unexpected components were needed for ISO and RIM, and one for MONU. Adding more unexpected components did not improve the fit, indicating that N- and U-PLS/RBL algorithms model the profiles of the interferences using one or two principal components. Both algorithms allow for a good prediction of herbicide concentrations in samples with potential interferences (Figs. 6C and 6D), suggesting that PLS/RBL does not require trilinearity to be strictly fulfilled to resolve very complex systems. According to the statistical results (Fig. 6E and Table 3), U-PLS/RBL renders prediction of better quality than N-PLS/RBL.

As regards the LODs obtained when U-PLS and U-PLS/RBL were applied to validation and test samples, respectively, it can be concluded that these values do not significantly differ. However, it should be taken into account that validation samples were processed using the complete data matrix, while the samples with potential interferences were investigated in selected regions. This latter procedure favors the results but makes it more tedious.

Real water samples

With the purpose of testing the applicability of the investigated method to real systems, the analysis of different kinds of waters was performed. In water bodies, herbicides are detected in a wide range of concentrations, generally in the order of part- and sub-part-per-billion levels. Therefore, in order to increase the sensitivity of the method, a preconcentration step

was carried out by employing C18 membrane-SPE, which proved to be an appropriate material.

Because the analyzed waters did not contain the studied herbicides, the samples were spiked, in duplicate, with the analytes, before the SPE procedure. It is important to recall that, in order to mimic a potential real situation, foreign compounds selected from the above analyzed group (TBZ, FBZ, MCPA or CBL) were added to each of these samples and a recovery study was carried out.

According to the previous results with artificial samples, U-PLS/RBL was the algorithm selected for the analysis of real samples. The good obtained results (Table 4) suggest that the method overcome the problem of the presence of unexpected interferents from the background of the real samples. In addition, the statistical results shown in Table 3, with very good values for RMSEP and REP, do also support this conclusion. The attained LODs (in the order of 2 ng mL^{-1}) suggest that the presently developed methodology is well suited for the determination of the analytes in surface and undeground water samples which might be exposed to the studied herbicides. For its application to the specific case of drinking water samples, it would be easy to increase the preconcentration factor.

Conclusions

It is demonstrated that a simple and green chromatographic technique which combines photo-induced fluorescence detection and chemometric analysis is a powerful tool for the determination of urea herbicides, and represents a better alternative than the conventional univariate calibration technique. The advantage lies in the possibility of carrying out the quantification in the presence of foreign compounds which will produce a serious interference in traditional analysis. Thus, extraction and clean procedures are not necessary avoiding the use of toxic solvents. The systems formed by validation samples (without

foreign compounds) showed to be trilinear and the four assayed algorithms rendered excellent results. The fluorescence spectra of some compounds selected as potential interferences were very similar to those of the analyte photoproducts. This fact, in addition to the shifts of the bands among different runs, produced problems in the data treatment of this type of samples. Although acceptable results were obtained using N-PLS/RBL and MCR-ALS, U-PLS/RBL showed the best performance to quantify the herbicides even in the presence of the selected foreign compounds.

Acknowledgements

The authors gratefully acknowledge the Universidad Nacional de Rosario, Consejo Nacional de Investigaciones Científicas y Técnicas and Agencia Nacional de Promoción Científica y Tecnológica (Project 2010-0084) for financially supporting this work.

References

1 R. Carabias Martínez, E. Rodríguez Gonzalo, E. Herrero Hernández, J. Hernández Méndez, *Anal. Chim. Acta*, 2004, **517**, 71–79.

2 F. J. Benitez, F.J. Real, J. L. Acero, C. García, *Water Res*., 2007, **41,** 4073–4084.

3 L. Nitschke, W. Schüssler, *Chemosphere*, 1998, **36,** 35–41.

4 N. H. Spliid, B. Køppen, *Chemosphere*, 1998, **37,** 1307–1316.

5 R. Meffe, I. de Bustamante, *Sc. Total Environ.*, 2014, **481,** 280–295.

6 J. Fenoll, M. Martínez Menchón, G. Navarro, N. Vela, S. Navarro, *Chemosphere*, 2013, **91**, 571–578.

7 R. Loos, G. Locoro, S. Comero, S. Contini, D. Schwesig, F. Werres, P. Balsaa, O. Gans, S. Weiss, L. Blaha, M. Bolchi, B. M. Gawlik, *Water Res*., 2010, **44**, 4115–4126.

8 S. R. Sørensen, G. D. Bending, C. S. Jacobsen, A. Walker, J. Aamand, *FEMS Microbiol. Ecol.*, 2003, **45**, 1–11.

9 S. Parra, V. Sarria, S. Malato, P. Péringer, C. Pulgarin, *Appl. Catal. B Eviron.*, 2000, **27,** 153–168.

10 https://www.gov.uk/government/uploads/system/uploads/attachment_data/file/162165/defra-stats-observatory-indicators-da4.-120224.pdf (accessed April 2014).

11 L. Nitschke, W. Schüssler, *Chemosphere*, 1998, **36**, 35–41.

12 R. Loos, B.M. Gawlik, G. Locoro, E. Rimaviciute, S. Contini, G. Bidoglio, *Environm. Poll.*, 2009, **157**, 561–568.

13 A.E. Rosenbom, J. Kjær, P. Olsen, *Chemosphere*, 2010, **79**, 830–838.

14 W. Chu, Y. F. Rao, *Chemosphere*, 2012, **86**, 1079–1144.

15 S. D. Richardson, *Anal. Chem*., 2010, **82**, 4742–4774.

16 A. Coly, J. J. Aaron, *Talanta*, 1999, **49**, 107–117.

17 A. Muñoz de la Peña, M. C. Mahedero, A. Bautista Sánchez, *J. Chromatogr. A*, 2002, **950**, 287–291.

18 A. Muñoz de la Peña, M. C. Mahedero, A. Bautista Sánchez, *Talanta*, 2003, **60**, 279–285.

19 S. Irace-Guigand, E. Leverend, M.D.G. Seye, J. J. Aaron, *Luminescence*, 2005, **20**, 138–142.

20 G. N. Piccirilli, G. M. Escandar, F. Cañada Cañada, I. Durán Merás, A. Muñoz de la Peña, *Talanta*, 2008, **77**, 852–857.

21 P. A. Diaw, A. Maroto, O. M. A. Mbaye, M. D. Gaye Seye, L. Stephan, A. Coly, L. Deschamps, A. Tine, J. J. Aaron, P. Giamarchi, *Talanta*, 2013, **116**, 569–574.

22 K. S. Booksh, B. R. Kowalski, *Anal. Chem*., 1994, **66**, 782A–791A.

23 Å. Rinnan, J. Riu, R. Bro, *J. Chemom*., 2007, **21**, 76–86.

24 G. M. Escandar, N. M. Faber, H. C. Goicoechea, A. Muñoz de la Peña, A. C. Olivieri, R. J. Poppi, *Trends Anal. Chem*., 2007, **26**, 752–765.

25 A. C. Olivieri, *Anal. Chem*., 2008, **80**, 5713–5720.

26 P. Anastas, N. Eghbali, *Chem. Soc. Rev*., 2010, **39**, 301–312.

27 J. A. Linthorst, *Found Chem*., 2010, **12**, 55–68.

28 R. Bro, *Chemom. Intell. Lab. Syst*., 1997, **38**, 149–171.

29 J. Öhman, P. Geladi, S. Wold, *J. Chemom*., 1990, **4**, 135–146.

30 A. C. Olivieri, *J. Chemom*., 2005, **19**, 253–265.

31 R. Bro, *J. Chemom*., 1996, **10**, 47–61.

32 R. Tauler, *Chemometr. Intell. Lab. Syst*., 1995, **30**, 133–146.

33 S. A. Bortolato, J. A. Arancibia, G. M. Escandar, *Anal. Chem*., 2009, **81**, 8074–8084.

34 F. Cañada Cañada, J. A. Arancibia, G. M. Escandar, G.A. Ibañez, A. Espinosa Mansilla, A. Muñoz de la Peña, A. C. Olivieri, *J. Chromatogr*. A, 2009, **1216**, 4868–4876.

35 A. Mancha de Llanos, M. M. de Zan, M. J. Culzoni, A. Espinosa Mansilla, F. Cañada Cañada, A. Muñoz de la Peña, H. C. Goicoechea, *Anal. Bioanal. Chem*., 2011, **399**, 2123–2135.

36 M. J. Culzoni, R. Q. Aucelio, G. M. Escandar, *Anal. Chim. Acta*, 2012, **740**, 27–35.

37 www.iquir-conicet.gov.ar/descargas/mvc2.rar (accessed April 2014).

38 C. J. Miles, H. A. Moye, *Anal. Chem*., 1988, **60**, 220–226.

39 A. Bautista, J. J. Aaron, M. C. Mahedero, A. Muñoz de la Peña, *Analusis*, 1999, **27**, 857–863.

40 E. Pramauro, E. Pelizzetti, Surfactants in Analytical Chemistry. Applications of Organized Amphiphilic Media. S. G. Weber (Ed.), Wilson & Wilson´s Comprehensive Analytical Chemistry (Elsevier, Amsterdam, The Netherlands, 1996) vol XXXI, Ch 4.

41 J. J. Aaron, A. Coly, *Analyst*, 1996, **121**, 1545–1549.

42 R. Bro, H. A. L. Kiers, *J. Chemom*., 2003, **17**, 274–286.

43 P. C. Damiani, I. Durán Merás, A. García Reiriz, A. Jiménez Jirón, A. Muñoz de la Peña, A. C. Olivieri, *Anal. Chem*., 2007, **79**, 6949–6958.

44 A. G. González, M. A. Herrador, A. G. Asuero, *Talanta*, 1999, **48**, 729–736.

45 W. Windig, J. Guilment, *Anal. Chem*., 1991, **63**, 1425–1432.

46 D. M. Haaland, E. V. Thomas, *Anal. Chem*., 1988, **60**, 1193–1202.

47 G. M. Escandar, H. C. Goicoechea, A. Muñoz de la Peña, A. C. Olivieri, *Anal. Chim. Acta*, 2014, **806**, 8–26.

Table 1 Composition of the samples used in the calibration, validation and test sets[a]

Calibration			Validation			Test[b]		
ISO	RIM	MONU	ISO	RIM	MONU	ISO	RIM	MONU
1.96	4.98	1.50	3.67	0.41	0.42	3.67	0.41	0.42
0.82	4.00	2.37	1.22	1.22	0	1.22	1.22	0
0.82	4.00	0.62	2.45	3.88	1.04	2.45	3.88	1.04
0.82	1.02	2.37	1.63	3.06	1.46	1.63	3.06	1.46
3.10	4.00	2.37	3.47	0.82	0.83	3.47	0.82	0.83
0.82	1.02	0.62	1.39	1.43	0	1.39	1.43	0
0	2.49	1.50	2.24	4.08	1.21	2.24	4.08	1.21
3.10	1.02	2.37	0	2.04	2.91	0	2.04	2.91
1.96	2.49	3.00	1.80	2.86	1.87	1.80	2.86	1.87
3.10	1.02	0.62	2.86	3.47	0.42	2.86	3.47	0.42
1.96	2.49	1.50	1.02	0	2.50	1.02	0	2.50
3.92	2.49	1.50	2.65	2.45	2.29	2.65	2.45	2.29
1.96	2.49	0				3.06	3.26	1.87
3.10	4.00	0.62				0.82	0	2.58
1.96	0	1.50				2.57	1.83	2.08
						0	2.24	2.83

[a] Concentrations are given in μg mL^{-1}. [b] In addition to the analytes, these test samples contain other agrochemicals selected as potential interferents (see text).

Table 2 Instrumental and chemical parameters

	Values/reagents
Mobile phase (isocratic regime)	Acetronitrile/sodium citrate (pH=6)/methanol (55:40:5, v/v)
Column	Zorbax SB-C18, 4.6×150 mm, 5 µm
Volumetric flow-rate (mL min^{-1})	1
Scanning speed (nm/s)	14400
Response time (s)	0.0125
Temperature	Room temperature
Surfactant in samples	0.011 mol L^{-1} HTAC
Injection volume (µL)	200
Time range (min)	From 0 to 4
Emission range (nm)	From 288 to 460
Excitation wavelength (nm)	272
Excitation/emission slits (nm)	10/10
Photomultiplier gain	800 V
Calibration ranges (µg mL^{-1})	ISO (from 0 to 4); RIM (from 0 to 5); MONU (from 0 to 3).

Table 3 Statistical results for the studied herbicides in samples without unexpected constituents (validation set), with MCPA, TBZ, FBZ, and CBL as potential interferents (test set), and in spiked water samples using ET-PIFMs and different chemometric algorithms[a]

	PARAFAC			MCR-ALS			N-PLS			U-PLS		
	ISO	RIM	MONU	ISO	RIM	MONU	ISO	RIM	MONU	ISO	RIM	MONU
Validation set												
RMSEP[b]	0.18	0.17	0.12	0.10	0.24	0.16	0.19	0.24	0.10	0.19	0.19	0.11
REP[c]	9.1	7.0	8.0	4.9	9.4	10.4	9.8	9.6	6.6	9.7	7.8	7.0
LOD[d]	0.25	0.18	0.15	0.64	0.29	0.23	0.29	0.12	0.10	0.18	0.12	0.10
Test set												
RMSEP[b]	0.33	0.59	0.42	0.43	0.61	0.13	0.21	0.39	0.13	0.19	0.26	0.12
REP[c]	17	23	28	22	24	8.8	11	16	8.4	9.7	10	8.2
LOD[d]	[e]	[e]	[e]	[e]	[e]	[e]	0.16	0.28	0.26	0.15	0.12	0.09
Real waters[f]												
RMSEP[b]										1.1×10^{-3}	1.9×10^{-3}	1.4×10^{-3}
REP[c]										2.7	3.9	4.8
LOD[d]										2.9×10^{-3}	2.4×10^{-3}	1.7×10^{-3}

[a] In validation samples the complete data matrix was used, while in both test and water samples partial chromatographic and time regions were selected for each analyte (see text). [b] RMSEP (μg mL^{-1}), root-mean-square error of prediction. [c] REP (%), relative error of prediction. [d] LOD (μg mL^{-1}), limit of detection calculated according to ref. 47. [e] Not reported. [f] The results refer to five different water samples before SPE. For comparison, the RMSEP and LOD units are also given in μg mL^{-1}.

Table 4 Recovery study of mixtures of rimsulfuron, monuron and isoproturon in spiked water samples using ET-PIFMs and U-PLS/RBL[a]

	ISO			RIM			MONU		
	Taken	Found[b]	Rec	Taken	Found[b]	Rec	Taken	Found[b]	Rec
River water[c]	0.0356	0.0365(7)	103	0.0510	0.0529(4)	104	0.0156	0.0157(1)	101
Tap water[d]	0.0254	0.0240(1)	94	0.0204	0.0196(3)	96	0.0312	0.0292(3)	94
Underground water[e]	0.0458	0.0464(8)	101	0.0306	0.0178(3)	91	0.0520	0.0509(2)	98
Underground water[f]	0.0102	0.0112(3)	110	0.0102	0.0081(1)	79	0.0364	0.0348(3)	96
Underground water[g]	0.0306	0.0311(1)	102	0.0254	0.0262(1)	103	0.0104	0.0100(1)	96

[a] Concentrations are given in μg mL^{-1}, and recoveries (Rec) in percentages. [b] Mean of duplicates. Standard deviation between parentheses corresponds to the last significant figure. [c] From Paraná river (Santa Fe, Argentina). [d] From Funes City (Santa Fe, Argentina). [e] From Funes City (Santa Fe, Argentina). [f] From San Genaro (Santa Fe, Argentina). [g] From Venado Tuerto (Santa Fe, Argentina).

Figure captions

Fig. 1 Chemical structures of the investigated herbicides and other agrochemicals.

Fig. 2 Normalized emission fluorescence spectra of ISO (blue line), RIM (green line), and MONU (red line) photoproducts (A), and those of MCPA, TBZ, FBZ and CBL after irradiation under the used experimental conditions (B).

Fig. 3 (A) Three-dimensional plot of a typical chromatogram of a sample containing the studied herbicides and (B) the corresponding two-dimensional contour plot. (C) Two-dimensional contour plot of the chromatogram of a sample containing the studied herbicides and additional agrochemicals selected as potential interferent agents. Concentrations are as follows (all in μg mL^{-1}): ISO, 2.45; RIM, 3.88; MONU, 1.04; MCPA, 7.00; TBZ, 0.31; FBZ, 0.040; CBL, 0.80. The color bars in (B) and (C) indicate the vertical scale (in arbitrary PIF units).

Fig. 4 Elution profiles of a typical calibration sample (black solid line; C_{RIM} = 4.98 μg mL^{-1}, C_{MONU} = 1.50 μg mL^{-1} , C_{ISO} = 1.96 μg mL^{-1}), a typical validation sample (blue dashed line; C_{RIM} = 4.08 μg mL^{-1}, C_{MONU} = 1.21 μg mL^{-1}, C_{ISO} = 2.24 μg mL^{-1}), and a test sample (red dashed line; C_{RIM} = 3.06 μg mL^{-1}, C_{MONU} = 1.46 μg mL^{-1}, C_{ISO} = 1.63 μg mL^{-1}, C_{MCPA} = 7.00 μg mL^{-1}, C_{TBZ} = 0.31 μg mL^{-1}, C_{FBZ} = 0.04 μg mL^{-1}, C_{CBL} = 0.80 μg mL^{-1}). λex/λem = 272/345 nm. Vertical lines serve as guide for the eye.

Fig. 5 Plots for ISO (triangle), RIM (circle), and MONU (square) predicted concentrations in validation samples as a function of the nominal values using (A) PARAFAC, (B) MCR-ALS, (C) N-PLS, and (D) U-PLS. Solid lines indicate the perfect fits. (E) Elliptical joint regions (at 95 % confidence level) for slope and intercept of the regression of PARAFAC (gray line),

MCR-ALS (orange line), N-PLS (pink line), and U-PLS (black line). Black point in (E) marks the theoretical (intercept = 0, slope = 1) point.

Fig. 6 Plots for ISO (triangles), RIM (circles), and MONU (squares) predicted concentrations in test samples as a function of the nominal values using (A) PARAFAC, (B) MCR-ALS, (C) N-PLS, and (D) U-PLS. Solid lines indicate the perfect fits. (E) Elliptical joint regions (at 95 % confidence level) for slope and intercept of the regression of PARAFAC (gray line), MCR-ALS (orange line), N-PLS (pink line), and U-PLS (black line). Black point in (E) marks the theoretical (intercept = 0, slope = 1) point.

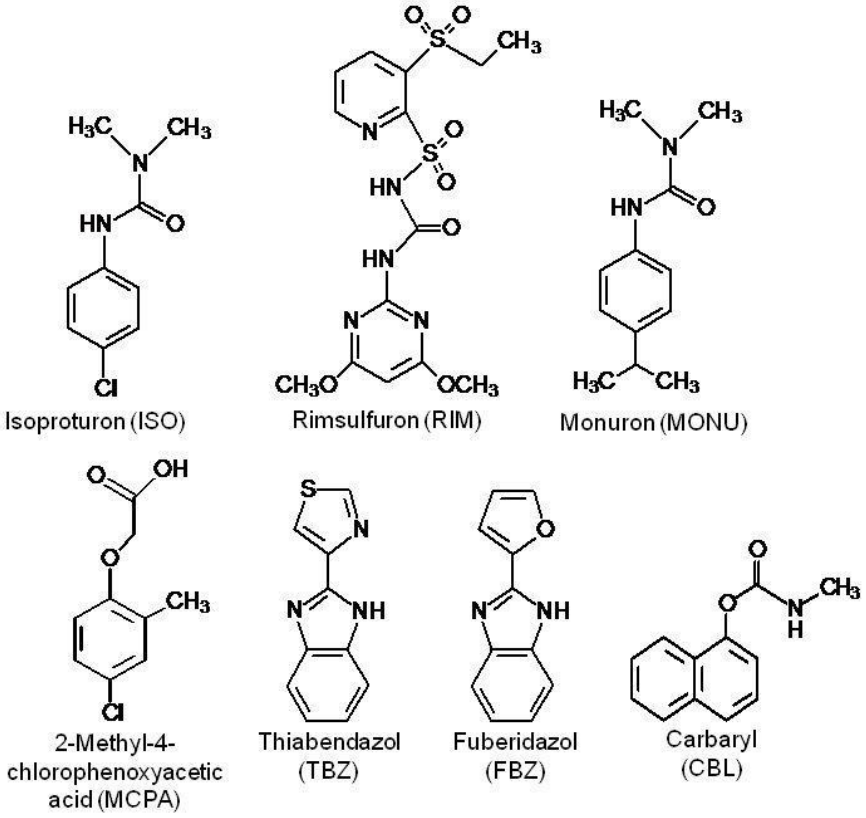
Isoproturon (ISO)
Rimsulfuron (RIM)
Monuron (MONU)
2-Methyl-4-chlorophenoxyacetic acid (MCPA)
Thiabendazol (TBZ)
Fuberidazol (FBZ)
Carbaryl (CBL)

FIGURE 1

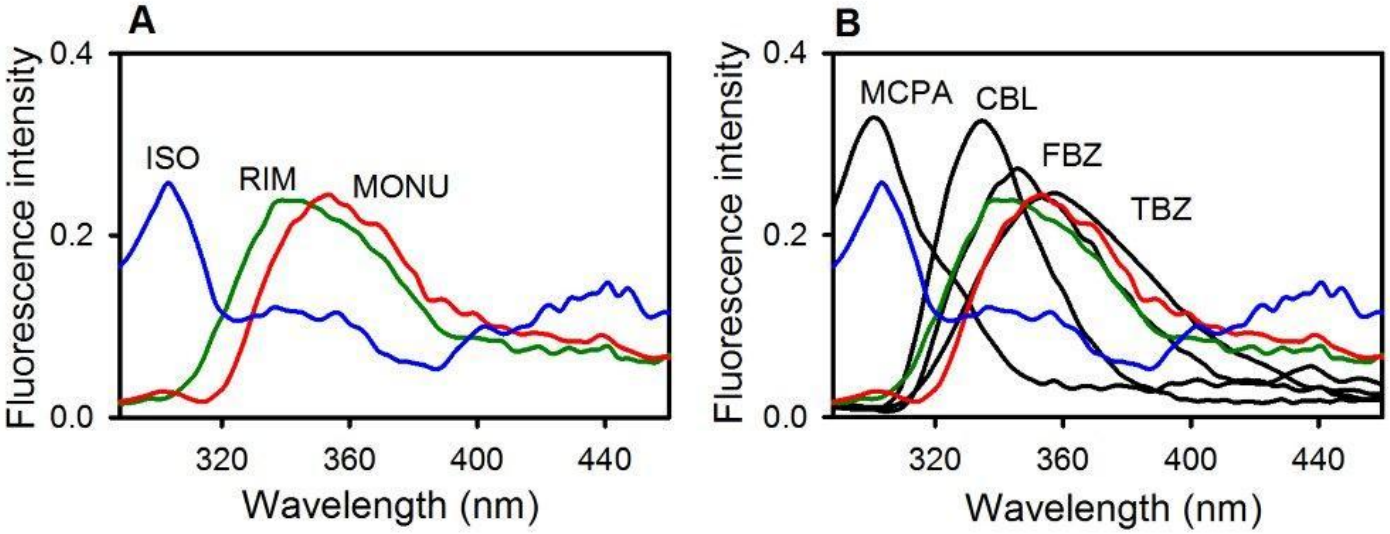
A
Fluorescence intensity
0.4
0.2
0.0
ISO
RIM
MONU
320
360
400
440
Wavelength (nm)
B
Fluorescence intensity
0.4
0.2
0.0
MCPA
CBL
FBZ
TBZ
320
360
400
440
Wavelength (nm)

FIGURE 2

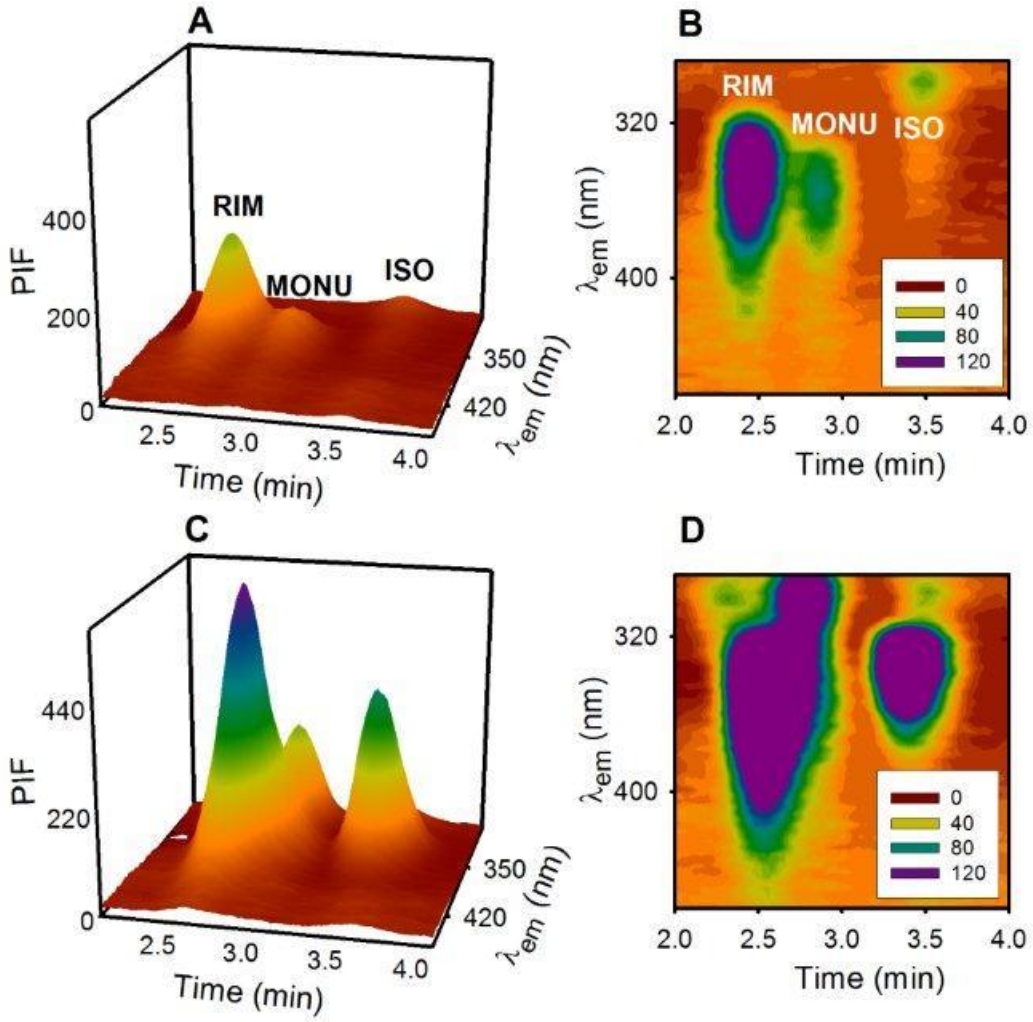
A
RIM
MONU
ISO
PIF
400
200
0
2.5
3.0
3.5
4.0
Time (min)
350
420
λem (nm)
B
RIM
MONU
ISO
320
400
λem (nm)
0
40
80
120
2.0
2.5
3.0
3.5
4.0
Time (min)
C
PIF
440
220
0
2.5
3.0
3.5
4.0
Time (min)
350
420
λem (nm)
D
320
400
λem (nm)
0
40
80
120
2.0
2.5
3.0
3.5
4.0
Time (min)

FIGURE 3

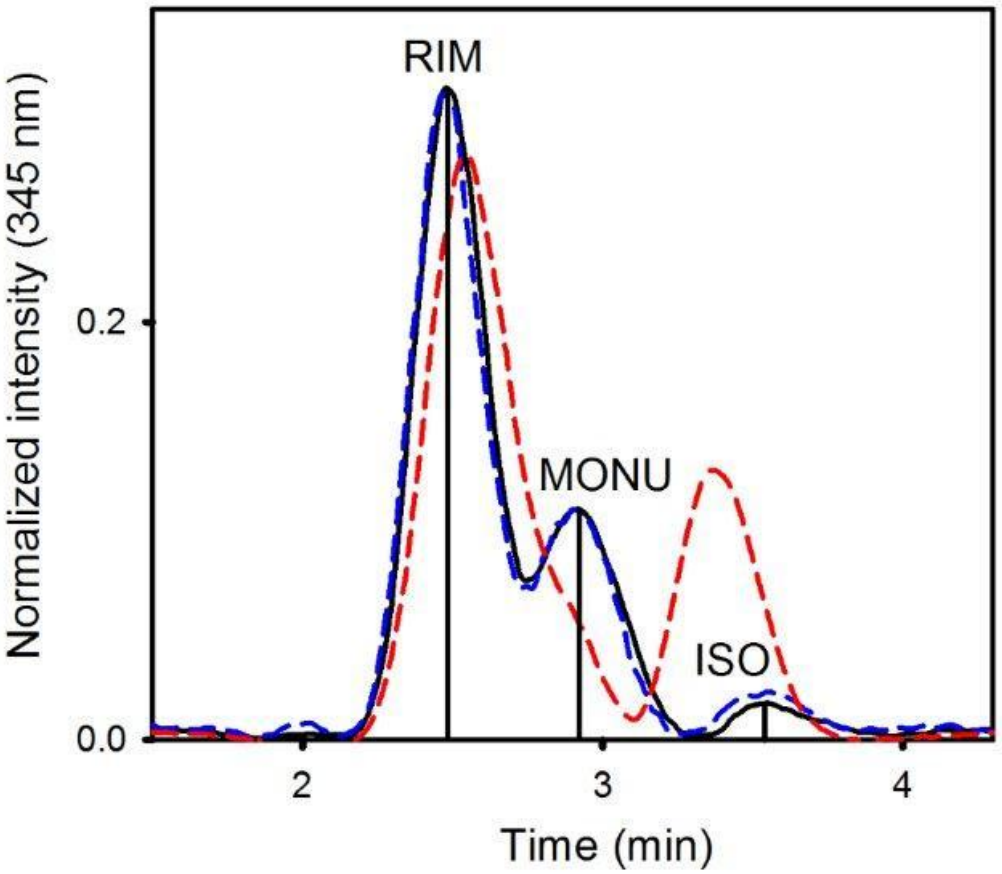

FIGURE 4

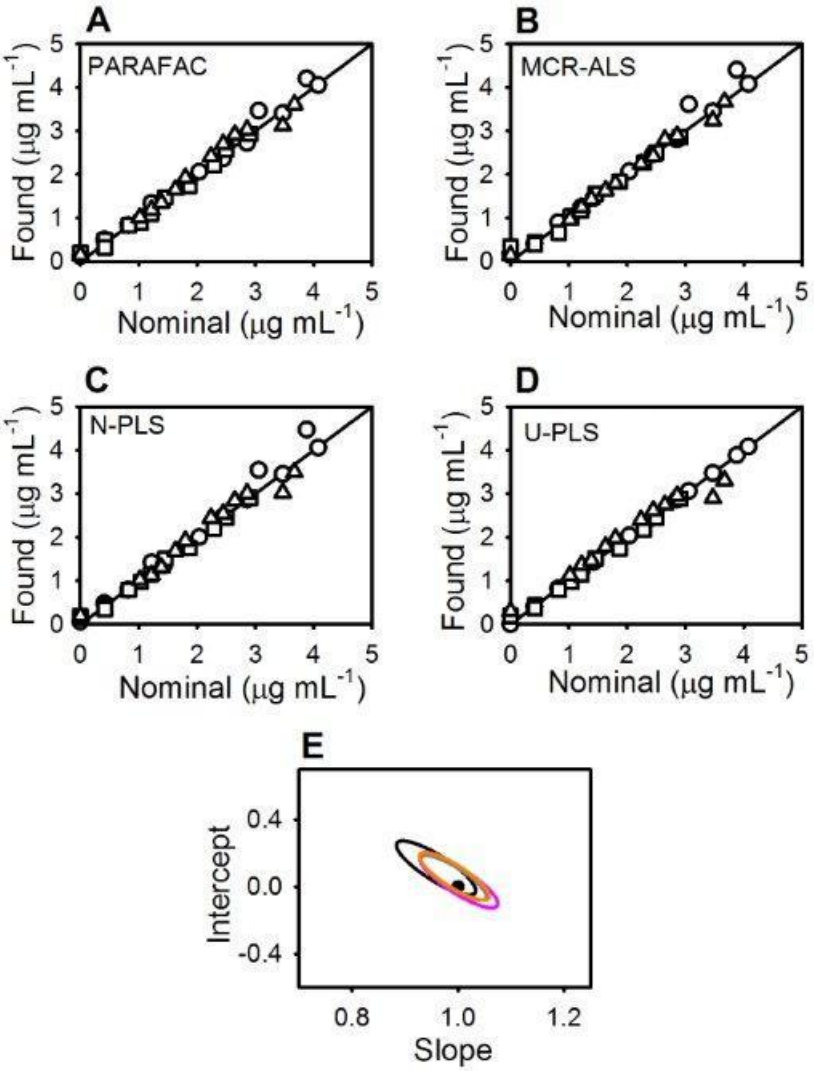
A
PARAFAC
B
MCR-ALS
C
N-PLS
D
U-PLS
Found (μg mL-1)
Nominal (μg mL-1)
0
1
2
3
4
5
E
Intercept
0.4
0.0
-0.4
0.8
1.0
1.2
Slope

FIGURE 5

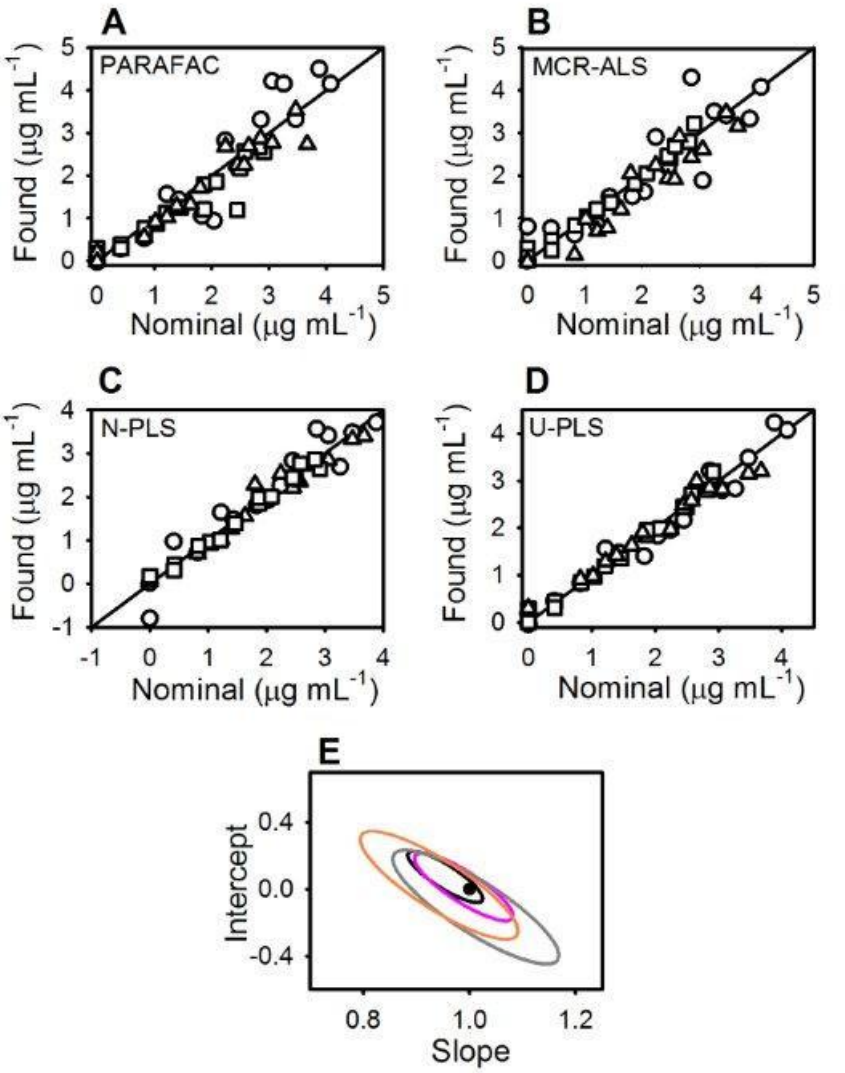
A
PARAFAC
Found (μg mL-1)
Nominal (μg mL-1)
B
MCR-ALS
Found (μg mL-1)
Nominal (μg mL-1)
C
N-PLS
Found (μg mL-1)
Nominal (μg mL-1)
D
U-PLS
Found (μg mL-1)
Nominal (μg mL-1)
E
Intercept
Slope

FIGURE 6